INSTITUTE OF PHYSICS PUBLISHING PHYSICS IN MEDICINE AND BIOLOGY

Phys. Med. Biol. **46** (2001) 1695–1706 www.iop.org/Journals/pb PII: S0031-9155(01)15357-1

Intensity modulated irradiation of a thorax phantom: comparisons between measurements, Monte Carlo calculations and pencil beam calculations

Wolfram U Laub[1], **Annemarie Bakai and Fridtjof Nüsslin**

Department of Medical Physics, University of Tübingen, Germany

Received 10 July 2000, in final form 17 April 2001

Abstract

The present study investigates the application of compensators for the intensity modulated irradiation of a thorax phantom. Measurements are compared with Monte Carlo and standard pencil beam algorithm dose calculations. Compensators were manufactured to produce the intensity profiles that were generated from the scientific version of the KonRad IMRT treatment-planning system for a given treatment plan. The comparison of dose distributions calculated with a pencil beam algorithm, with the Monte Carlo code EGS4 and with measurements is presented. By measurements in a water phantom it is demonstrated that the method used to manufacture the compensators reproduces the intensity profiles in a suitable manner. Monte Carlo simulations in a water phantom show that the accelerator head model used for simulations is sufficient. No significant overestimations of dose values inside the target volume by the pencil beam algorithm are found in the thorax phantom. An overestimation of dose values in lung by the pencil beam algorithm is also not found. Expected dose calculation errors of the pencil beam algorithm are suppressed, because the dose to the low density region lung is reduced by the use of a non-coplanar beam arrangement and by intensity modulation.

1. Introduction

With the concept of intensity modulated radiation therapy (IMRT), high and homogeneous doses can be delivered to almost arbitrary target volumes. Simultaneously, it succeeds in limiting damage to normal tissue, which improves tolerance of radiation therapy. Naturally, for this to be achieved it is necessary to calculate dose distributions as exactly as possible (ICRU 1987, Mohan 1997, Nahum 1997).

Almost all IMRT treatment-planning systems employ pencil beam algorithms, because they use iterative optimization procedures and therefore need fast dose calculation algorithms

[1] Now at William Beaumont Hospital, Department of Radiation Oncology, 3601 West 13 Mile, Royal Oak, MI 48073, USA. E-mail: wlaub@beaumont.edu

0031-9155/01/061695+12$30.00

(Mohan 1998, Bortfeld *et al* 1993, Schulze *et al* 1997, Ahnesjö 1991, Ahnesjö *et al* 1992). It is difficult to modify pencil beams for patient shape and heterogeneity. For expedience, empirical scaling methods are employed. Because the energy transport of secondary electrons, which may travel up to a few centimetres in water, is not taken into account by scaling methods, dose calculations with pencil beam algorithms lead to errors near surfaces and inhomogeneities. The Monte Carlo code EGS4 (Nelson *et al* 1985) (Electron Gamma Shower, Version 4) uses exact interaction probabilities of electrons and photons. To verify Monte Carlo dose calculations several authors performed measurements in water phantoms and in various solid state phantoms (Laub *et al* 1998, Lu *et al* 1998, De Marco *et al* 1998). The experiments were designed with the emphasis on the missing-tissue effect near surfaces, the re-buildup effect underneath low-density inhomogeneities and variations of dose values through deviations in the atomic number of different materials. In all cases Monte Carlo calculations and measurements were in agreement. Contrary to this, calculations made with conventional dose calculation algorithms showed errors when compared with measurements of up to 15% in proximity of surfaces and inhomogeneities.

In the irradiation of the mediastinum, lung and thus low density regions are situated adjacent to the target volume. As stated above, errors must be expected in the presence of such inhomogeneities (Lu *et al* 1998). In IMRT dose can be tailored to the geometry of the target and/or there can be a high dose gradient at the edge of the treatment volume. Consequently, dose calculation errors could have a great effect on the tumour control and the advantages of an IMRT treatment in the thorax region could be diminished or even undermined due to dose calculation inaccuracies. Conversely, IMRT has the potential to reduce the dose to organs at risk compared to conventional treatment planning. Therefore dose calculation errors in lung could also be smaller and no longer of clinical relevance.

This study compares measurements, Monte Carlo calculations and pencil beam calculations of an IMRT treatment plan. The IMRT treatment plan was designed in an inhomogeneous physical thorax phantom. Compensators were manufactured to produce the intensity profiles that were generated with the scientific predecessor version 1.2 beta of the KonRad IMRT treatment-planning system (MRC Systems, 1997) (Bortfeld *et al* 1993, 1997, Preiser *et al* 1997). Measurements were performed for comparison with EGS4 calculations in a water phantom as well as in the thorax phantom. For these calculations, EGS4 was linked to the treatment-planning system VOXELPLAN (DKFZ-Heidelberg). The results of the measurements and EGS4 calculations were compared to the original fluence profiles of the designed IMRT treatment plan and to the dose distribution that was calculated with the pencil beam algorithm of KonRad in the thorax phantom.

2. Methods

2.1. IMRT treatment planning in KonRad

For this study a lung tumour was defined in a thorax phantom. A prescription dose of 70 Gy was set for the defined tumour; a dose of 50 Gy was prescribed to the defined planning target volume (PTV). Five non-coplanar beams of 6 MV were arranged in angles of (gantry, couch): (5, 0), (40, 40), (164, 30), (205, 0) and (310, 0) degrees. The optimization of the dose distribution employed dose–volume histogram (DVH) constraints, and quadratic overdose and underdose constraints. The resolution of the grid of the resulting intensity profiles was 9×9 mm^2 at isocentre distance 100 cm. The finite-size pencil beam algorithm used in KonRad is described elsewhere (Bortfeld *et al* 1993).

2.2. Dose calculation in VOXELPLAN with EGS4

To perform accurate dose calculations of treatment plans with the EGS4 code an accelerator head model is necessary which gives the parameters of electrons and photons emitted by a clinical accelerator. A full phase-space file of a 15×15 cm^2 open field was used to start Monte Carlo (MC) histories. This file resulted from BEAM (Roger *et al* 1995) simulations of an Elekta SL 20 linear accelerator and was calculated at a distance of 67.2 cm from the electron source, which is exactly the distance to the block tray of the SL 20. To match the 9×9 mm^2 resolution of the grid of the intensity profiles calculated in KonRad at isocentre distance 100 cm, all electrons and photons of the phase-space file were organized in a 6×6 mm^2 grid. Intensity modulated fields were then simulated with the number of MC histories started from each element of this grid proportional to the fluence through that element as calculated in KonRad. Consequently, scatter or beam hardening from the compensators was not accounted for in the MC simulations. An inclusion of compensators in BEAM simulations would be possible because the compensator profiles are known before starting the MC simulation. However, a beam modifier model would need further investigation and is beyond the scope of this paper. The CT cube in VOXELPLAN is given by slices of 256×256 pixels. The volume of the CT voxels is (pixel size) $\times$ (slice distance), with a slice distance of 0.5 cm and pixel dimensions of 0.2×0.2 cm^2 for the CT cube of the thorax phantom. For Monte Carlo simulations the CT numbers of these voxels (in Hounsfield units) are converted into mass densities by the same function as used in VOXELPLAN. Thresholds of the CT numbers are set to distinguish a small number of different media or tissues. Simulations in the thorax phantom distinguished the media Alderson lung, Alderson muscle, bone and air. In contrast to conventional dose calculation algorithms, differences in the composition and therefore even in the effective atomic number Z of media are regarded. To save computation time, the body outline of patients or phantoms is used to set the medium of all voxels outside the drawn contour to vacuum. Contours around organs at risk can be used to distinguish further media inside patients and phantoms. The dose cube in VOXELPLAN is given by slices of 128×128 pixels, with pixel dimensions of 0.4×0.4 cm^2 for the dose cube of the thorax phantom. Calculated dose cubes can be viewed in the program module VIRTUOS. The dose cube resolution was identical for Monte Carlo and pencil beam calculations.

For the calculation of dose distributions with EGS4, between 150 and 250 million single events were simulated. The statistical accuracy of the simulations was about 0.5–1% near the isocentre of the calculated treatment plan. The electron and photon cutoffs ECUT and PCUT were set to 611 keV and 100 keV, the electron and photon production thresholds AE and AP were set to 521 keV and 10 keV. The value of the parameter ESTEPE (maximum fractional energy a charged particle can lose per step) was settled to 4%. These parameters were found by Lovelock *et al* (1995) to be those of the fastest trial. Simulations were run on a DEC Alpha dual processor machine (533 MHz) with calculation times between 10 h and 20 h.

2.3. Verification measurements

To produce the intensity profiles that resulted from the optimization in KonRad for measurements at the Elekta SL 20 linear accelerator, compensators were manufactured with a CNC machine. The compensator thickness was calculated for each element of the intensity profile by using the average attenuation coefficient of the photon energy spectrum that resulted from the phase-space file calculated with BEAM. As a result of IMRT optimizations, very high fluence values sometimes occur for single elements. For the IMRT plan used in this study the high fluence values were always situated at the edges of the field, so they did not affect dose

values in the high dose region. These element values were set in order to limit the compensator thickness to a maximum of 6 cm. In building each compensator, parallel holes were drilled into a square MCP 96 block. Afterwards, tracks were milled in one direction. Residual islands between the tracks were finally broken off. It was not possible to account for the divergence of the 6 MV photon beam by drilling diverging holes into the blocks.

In order to confirm the accuracy of the intensity modulation produced by the compensators, two dose measuring methods were used. First, water phantom measurements were performed with a diamond detector. Profiles with different offsets and perpendicular to the central beam axis were measured with each compensator as beam modifier. The diamond detector was placed at dose maximum $d_{\max} = 1.3$ cm and at 5 cm, 10 cm and 20 cm surface distance with a SSD of 100 cm. Second, CEA TVS EP films were positioned in a water equivalent solid state phantom perpendicular to the central beam axis and at dose maximum. Measured profiles for each beam were compared with the input fluence profiles from KonRad because it was not possible to calculate the dose distribution of a given intensity modulated beam in a water phantom. The comparison of calculated fluence values with measured dose values gives an approximate estimate of the accuracy of manufactured compensators. Additionally, EGS4 dose calculations were performed in a water phantom and compared to dose measurements.

Finally, CEA films and thermoluminescence dosimeters (TL-100, Harshaw) were used to measure the dose distribution produced by the five intensity modulated beams of the treatment plan in the thorax phantom. Measurements were compared to the dose distribution calculated with EGS4 and with the finite-size pencil beam algorithm of KonRad.

3. Results and discussion

3.1. Measurements and Monte Carlo calculations in homogeneous phantoms

Above the minimum level of measured dose values, input fluence values from KonRad show good agreement with all measurements performed in a water phantom or in a homogeneous solid state phantom (figure 1). However, deviations can be noticed at regions of low fluence. In part, this is due to the fact that the scientific version of KonRad used does not account for transmission through the compensators. In addition, the primary fluence is compared to measured dose at depth in a water phantom. The dose in the water phantom will include contributions from photons scattered in water and secondary electrons produced in the medium from regions of high intensities. The scientific version of KonRad used in this study did not allow specification of a minimum value for fluence profile elements of a rectangular field. For the presented treatment plan the effect of transmission through compensators on the final dose distribution will be discussed.

Film and diamond detector measurements agree to within $\pm 3\%$, and at regions of high dose gradients profiles are displaced by less than ± 2 mm (figure 1). Consequently, film measurements, which are much easier to perform, would be sufficient to check the quality of compensators. Independent checks would be required for absolute doses. Measurements and dose profiles calculated with EGS4 in a water phantom also agree. The maximum deviation is about 5% or about ± 2 mm at regions of high dose gradients but is well within $\pm 3\%$ for most points. A value for the minimal transmission of photons through the compensators was set and accounted for in the presented MC simulation. Compared to the measured transmission the value set in the MC simulation is low and therefore was increased slightly for further EGS4 simulations. The underestimation of the transmission in the MC simulation does not effect dose values above 25%.

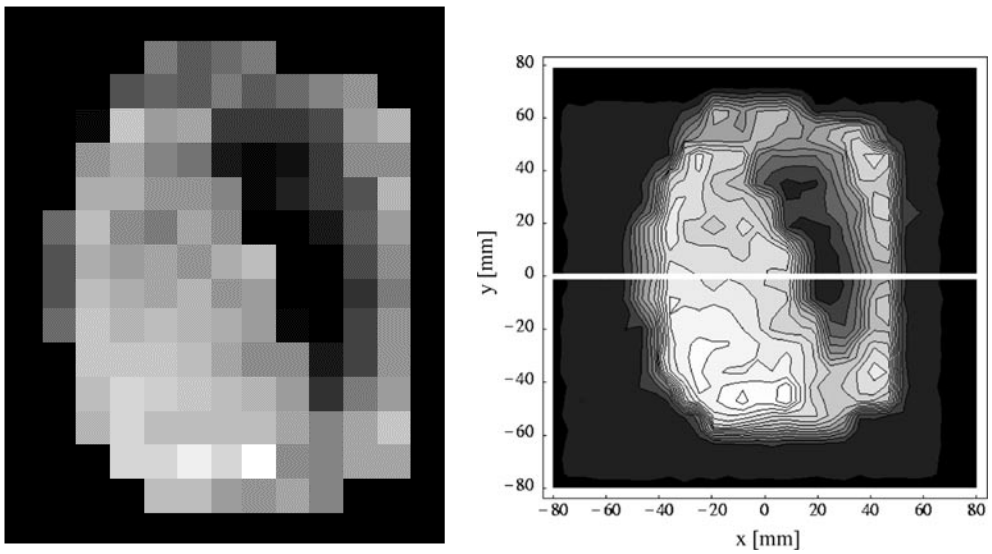

(a)

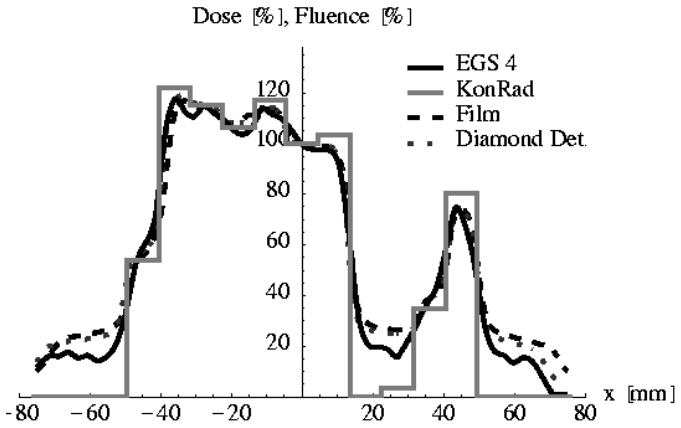

(b)

Figure 1. (a) Fluence matrix of beam 1 as resulting from the optimization process in KonRad for a five beam IMRT treatment plan (left) and dose values of beam 1 as calculated at dose maximum in a water phantom with EGS4 (right). The white line in the EGS4 calculation shows the position of the profile displayed in figure 1(b). (b) Profile of beam 1 at dose maximum and at central beam axis as calculated with EGS4 and measured with film and a diamond detector in a water phantom. The fluence values given by KonRad are displayed for comparison. It can be noticed that KonRad postulates fluence values within the field of almost zero (here at position $x = 15$ mm). The shown EGS4 simulation accounts for a transmission of the compensator of beam 1 which is a little too low compared to the measured transmission. This was corrected for further EGS4 simulations.

In spite of the non-divergent quality of the compensators, the agreement between measurements and dose profiles calculated with EGS4 is independent of the offset and the surface distance of the viewed profiles (figure 2). Most deviations caused by inaccuracies of the manufacturing were found to result from MCP 96 islands that were not completely removed and remained between milled tracks. Because of the good agreement between MC simulations and measurements it can be asserted that this compensator manufacturing method is suitable for

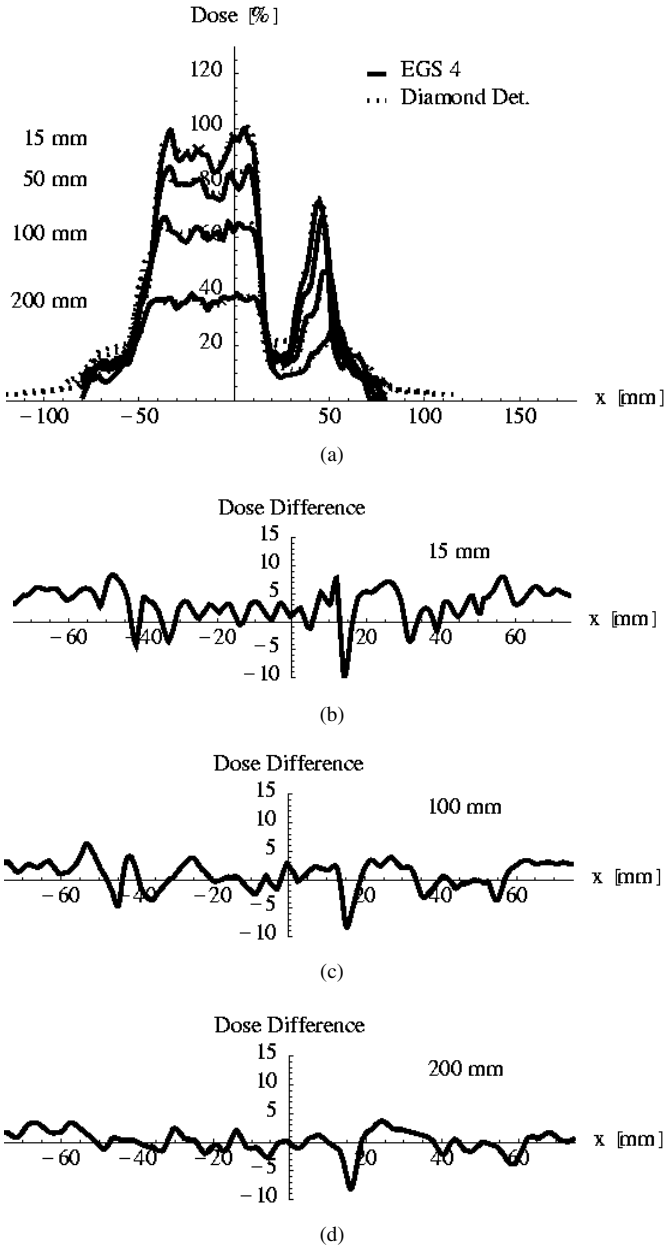

Figure 2. Profile of beam 1 at dose maximum depth and at 5, 10 and 20 cm surface distance with an offset of 9.1 mm as calculated with EGS4 and measured with a diamond detector. Differences between calculated and measured dose values are displayed for the dose maximum depth and for 10 cm and 20 cm surface distance.

producing given intensity profiles. The reasonably good agreement between fluence values from KonRad and measurements also confirms this assertion. Moreover, it is found that the method to account for intensity modulation during the MC calculations, by setting the number of histories in an element proportional to the fluence calculated from KonRad, does not lead

to recognizable errors, despite the omission of scatter as well as beam hardening from the compensators.

3.2. Measurements and Monte Carlo calculations in a thorax phantom

After all manufactured compensators were checked in a homogeneous phantom, verification was performed of the dose distribution in a thorax phantom as calculated by the KonRad pencil beam algorithm. For the experimental verification TLDs as well as CEA films were used. Both dosimetric methods were found to be time consuming and expensive. Calibration measurements were necessary in both cases. Films were cut to the exact shape of phantom slices and positioned between phantom slices. For the TLD measurements many TLDs had to be numbered and placed into holes of phantom slices. For comparison with calculated dose values, measured dose values were matched with the phantom anatomy. Moreover, the positioning and irradiation of the thorax phantom took about 2 h. This effort was rewarded by good agreement between film and TLD measurements; at least if the approximately 1% of TLDs with anomalous readings are neglected. TLD measurements were rejected if they were more than 50% higher than expected.

There is also good agreement between the EGS4 calculation of the dose distribution and the dose measurements (figure 3). Therefore, to verify the KonRad pencil beam calculations, the EGS4 calculation can be considered a substitute for measurements. In the following paragraphs the dose distributions of the EGS4 calculation and the pencil beam calculation are compared.

Our comparison of Monte Carlo and pencil beam calculations shows no significant deviations of dose values in lung or near the interface between the PTV and lung. The deviations found in figure 3 for $x' \approx 60$ to 80 mm are not situated in lung and are due to the transmission through the compensators that was accounted for in the MC calculation, but not in the pencil beam calculation. Accounting for the transmission through the compensators would increase dose values of the pencil beam calculation in this region and would therefore improve the agreement between MC and pencil beam calculation. An increase of fluence due to transmission for $x' \approx -60$ to -80 mm would potentially lead to higher dose values in lung in the pencil beam calculation than in the MC simulation. It is difficult to estimate the effect of an increase of fluence due to transmission on dose values in the high dose region. However, from figures 3 and 4, we believe that in our example, the lack of transmission in the pencil beam calculation has not greatly affected the high dose region.

For a CT slice at the isocentre, figure 4 displays the IMRT dose distributions as calculated with the KonRad pencil beam algorithm (left) and with EGS4 (right). The 95%, 80%, 60%, 30% and 10% isodose contours are displayed. In agreement with figure 3, the dose distributions show only slight differences in the PTV and in lung. Because the differences between the two dose distributions are small the dose–volume histograms are also similar (figure 5).

Some differences in dose distributions could be caused by the use of two different accelerator head models. Pencil beam algorithms use analytical functions to account for scattered photons and for electron contamination, while a full phase-space file from BEAM simulations was used in this investigation to start MC histories. However, differences caused by the use of two different accelerator head models should not be significant. Another explanation for the slight differences found are small humps in the KonRad profiles (figure 3), which result from the discrete grid of the finite-sized pencil beam kernels. As a consequence of these humps, the isodose lines of the pencil beam calculation are less smooth than the isodose lines of the MC simulation. Statistical inaccuracies of the presented MC calculation must only be considered for low dose values. In these regions, dose contributions are made by only one or two of all five beams, which results in fewer interactions per voxel than in high dose regions

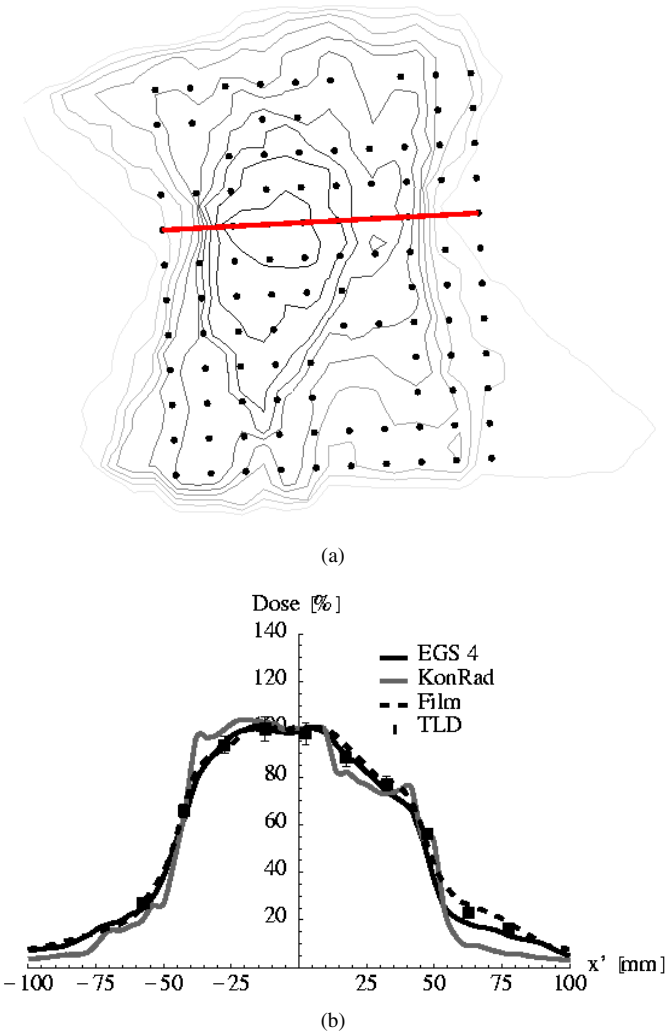

Figure 3. Profile of the dose distribution as calculated for a five-beam IMRT treatment plan with EGS4 and measured with film and TLDs in a thorax phantom. The profile of the dose distribution as calculated by a finite-size pencil beam algorithm in KonRad is displayed for comparison. The small humps that can be noticed result from the discrete grid of the finite-sized pencil beam kernels. The upper plot shows the position of the profile, the position of the holes used for TLD measurements and the dose distribution as measured with film.

and therefore in an decrease of the statistical accuracy. Fewer interactions per voxel also occur in low density regions like lung. However, the number of simulated histories was very high so that the statistical accuracy is better than 2% for all voxels. As discussed before, differences in the low dose region of lung are caused by the transmission that was accounted for in the MC simulation, but not in the pencil beam calculation. In addition, the MC simulation of secondary photon and electron transport leads to a broader penumbra in low density regions like lung as compared to the pencil beam calculation. Differences between the MC and pencil beam calculations arise in the 10% and 30% isodose lines of figure 4 and in the DVHs of lung for dose values below 30% due to a combination of these two effects (figure 5).

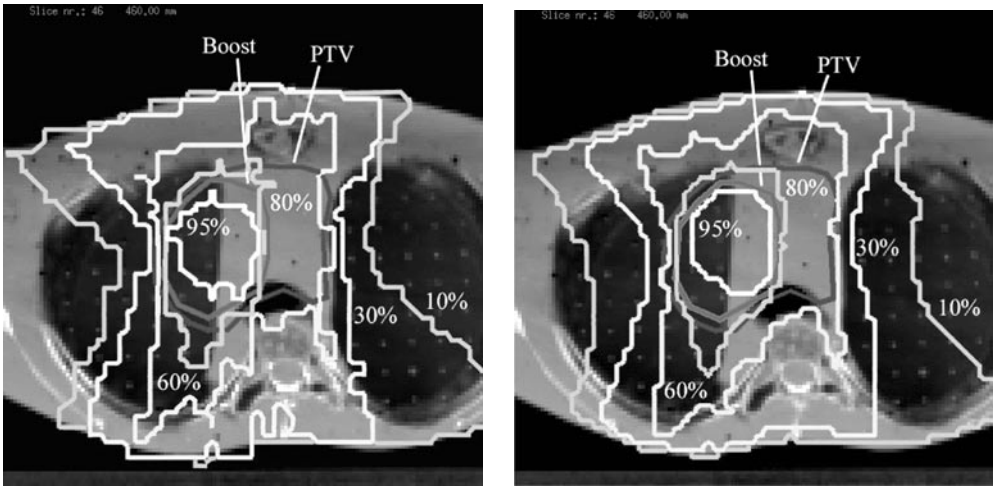

(a) (b)

Figure 4. Dose distribution of an IMRT treatment plan in the thorax region of a phantom as calculated with a pencil beam algorithm in KonRad (left) and with the EGS4 code (right).

The initially surprising agreement between pencil beam calculation and MC simulation is explained by three observations. First, the phantom lung volume has a homogeneous density. This is not true for real patients, where one finds voxels with lung tissue adjacent to voxels containing mostly air. As a consequence, there is no electron equilibrium in most regions of real human lung, which makes dose calculations more difficult and therefore decreases the accuracy of pencil beam calculations. Second, the selected beam directions were chosen to avoid dose in lung, which is a typical treatment planning objective. Some beams barely pass through lung and consequently dose calculation errors in lung and at the interface between lung and PTV are reduced. Third, with intensity modulation a further reduction of dose in lung and therefore of absolute dose calculation errors is attained. In other words, the increase of dose conformity in IMRT has the potential to suppress errors of pencil beam calculations in the presence of low density regions such as lung.

4. Summary and conclusion

The present study investigates the application of compensators for the intensity modulated irradiation of a thorax phantom. The comparison of measured dose distributions with dose distributions calculated with the EGS4 code in the VOXELPLAN treatment-planning system and with a pencil beam algorithm in the KonRad IMRT treatment planning system is presented.

A method to produce compensators is described. It is demonstrated that this method is suitable to create given intensity profiles. Monte Carlo simulations in a water phantom also show that the simple accelerator head model used for simulations is sufficient.

Differences between Monte Carlo and pencil beam calculations have been reported recently by Lu *et al* (1998) in the clinical example of a mediastinum treatment. The patient was irradiated with three coplanar beams. In the MC calculation the mean lung dose was lower by about 5–10% as compared to the pencil beam calculation. Because of the re-buildup effect, dose was also overestimated by the pencil beam algorithm near the interface between the PTV and lung. Consequently, the dose volume histograms of both dose distributions were very different.

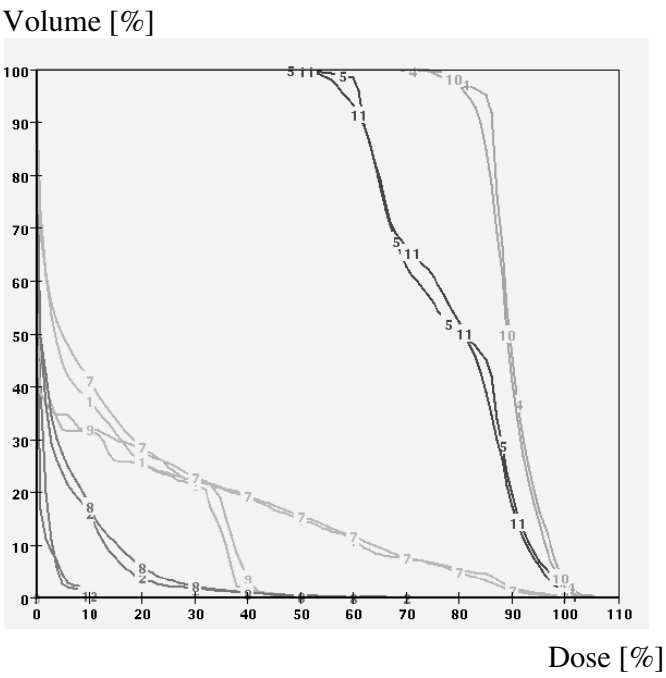

Figure 5. Dose–volume histogram of an IMRT treatment plan in the thorax region of a phantom. Lines number 7 and number 8 show the dose–volume histogram of lung as calculated with EGS4; line number 9 the one of the myelon; lines number 10 and number 11 show the dose–volume histogram of the target volumes. For comparison lines number 1 and number 2 show the dose–volume histogram of lung, line number 3 the one of the myelon and lines number 4 and number 5 show the dose–volume histograms of the target volumes of the pencil beam calculation in KonRad.

Contrary to the findings of Lu *et al* no significant overestimations of dose values inside the target volume by the pencil beam algorithm were found in the thorax phantom used in this study, in which the target volume was situated adjacent to low density inhomogeneities. An overestimation of dose values in lung by the pencil beam algorithm also was not found. It should be noted that a direct comparison can not be made because of major differences in the treatment planning approach. In this study a phantom was used compared to a patient dataset in Lu *et al* . Additionally, the expected errors of pencil beam calculations in the presence of low density regions can potentially be suppressed by the use of non-coplanar beam arrangements and/or intensity modulation, because these techniques have the ability to reduce the dose in organs at risk such as lung.

However, in this specific example the observation can be made that the pencil beam calculation proved to compare reasonably well with Monte Carlo calculations. Nevertheless, it should not be concluded that in IMRT the accuracy of pencil beam calculations is always sufficient and that the clinical relevance of Monte Carlo dose calculations is always smaller than in conventional treatment planning. It is difficult to draw any general conclusions from the pencil beam calculations in this study because of lack of transmission, because we are dealing with a phantom in our study, not with a patient dataset, and because efforts have been made with beam orientation to avoid the lung. As demonstrated by Laub *et al* (2000) there are still some clinical situations in IMRT in which it is possible that the inaccuracies of pencil beam algorithms are of clinical relevance. Inaccuracies of pencil beam algorithms can be of

clinical relevance in the head and neck region for example, where PTVs are in general small and where the treatment geometry is highly reproducible. In such situations the compensation of secondary electron disequilibrium, e.g. the loss of dose in the re-buildup areas, is possible by primary fluence (Laub *et al* 2000). Therefore, in some situations an accurate dose calculation can be of much more importance in IMRT than in conventional treatment planning, where losses of dose near low density volumes must be tolerated.

In the thorax region both Monte Carlo and pencil beam calculation accuracies are limited due to errors caused by intra-fraction variation of lung volume (Stromberg *et al* 2000). Treatment setup errors of real mediastinal patients are clinically more significant than the differences found in this study between the pencil beam and the MC dose calculation (Yan *et al* 1997). To minimize these errors some effort has been made already. A device for active breathing control was developed for example (Wong *et al* 1999). The approximations and simplifications made by the pencil beam calculation can therefore be justified by the advantage of shorter calculation times, which is an important issue of IMRT optimizations. However, the dose distribution of the optimized IMRT treatment plan should be verified with a more sophisticated dose calculation method to ensure that the clinical objectives are achieved. The influence of transmission depends on the shape of the calculated intensity profiles and could be more significant for treatment plans other than that presented. A possibility to set minimum fluence values for optimizations in IMRT treatment planning systems would therefore be desirable.

Acknowledgments

This work was in part supported by the Deutsche Krebshilfe. We are grateful to Laura Pisani, Carl Rowbotton and Markus Alber for their support. We are also grateful to MRC Systems for providing us with the scientific version 1.2 beta (1997) of the IMRT planning system KonRad. However, it should be noted that this version is not identical to the currently available commercial version of KonRad.

References

Ahnesjö A 1991 Dose calculation methods in photon beam therapy using energy deposition kernels *Thesis* University of Stockholm

Ahnesjö A, Saxner M and Trepp A 1992 A pencil beam model for photon dose calculation *Med. Phys.* **19** 263–73

Bortfeld T, Schlegel W and Rhein B 1993 Decomposition of pencil beam kernels for fast dose calculations in three-dimensional treatment planning *Med. Phys.* **20** 311–18

Bortfeld T, Stein J and Preiser K 1997 Clinically relevant intensity modulation optimization using physical criteria *Proc. 12th ICCR (Salt Lake City, UT, 1997)* pp 1–4

DeMarco J J, Solberg T D and Smathers J B 1998 A CT-based Monte Carlo simulation tool for dosimetry planning and analysis *Med. Phys.* **25** 1–11

ICRU 1987 Use of computers in external beam radiotherapy procedures with high-energy photons and electrons *ICRU Report 42*

Laub W, Alber M, Birkner M and Nüsslin F 2000 Monte Carlo dose calculation for IMRT optimization *Phys. Med. Biol.* **45** 1741–54

Laub W U, Alber M and Nüsslin F 1998 Verification of Monte Carlo photon dose calculations and comparison with pencil beam algorithms in the presence of tissue inhomogeneities *Radiother. Oncol.* **48** 123

Lovelock D M J, Chui C S and Mohan R 1995 A Monte Carlo model of photon beam used in radiation therapy *Med. Phys.* **22** 1387–94

Lu W, Chen-Shou C and Lovelock M 1998 A patient-specific Monte Carlo dose-calculation method for photon beams *Med. Phys.* **25** 867–78

Mohan R 1988 Dose calculations for radiation treatment planning *Monte Carlo Transport of Electrons and Photons* ed T M Jenkins *et al* (New York: Plenum) pp 549–73

Mohan R 1997 Why Monte Carlo? *12th Int. Conf. on the Use of Computers in Radiation Therapy* pp 16–18

Nahum A E 1997 Conformal therapy needs Monte Carlo dose computation *ESTRO Pre-Meeting Workshop on Challenges in Conformal Radiotherapy (Nice)* pp 1–11

Nelson W R, Hirayama H and Rogers D W O 1985 The EGS 4 Code System *SLAC Report* 265

Preiser K, Bortfeld T, Hartwig K, Schlegel W and Stein J 1997 A new program for inverse radiotherapy planning *Proc. 12th ICCR (Salt Lake City, UT, 1997)* pp 425–8

Rogers D W O, Faddegon B A *et al* 1995 12th BEAM: a Monte Carlo code to simulate radiotherapy treatment units *Med. Phys.* **22** 503–24

Schulze C, Pijpelink J *et al* 1997 3D photon dose calculation: from a scientific tool to routine planning *12th Int. Conf. on the Use of Computers in Radiation Therapy* pp 27–30

Stromberg J S, Sharpe M B, Kim L H, Kini V R, Jaffray D A, Martinez A A and Wong J W 2000 Active breathing control (ABC) for Hodgkin's disease: reproduction in normal tissue irradiation with deep inspiration and implications for treatment *Int. J Radiat. Oncol. Biol. Phys.* **48** 797–806

Wong J *et al* 1999 The use of active breathing control (ABC) to reduce margin for breathing motion *Int. J Radiat. Oncol. Biol. Phys.* **44** 911–19

Yan D *et al* 1997 Adaptive modification of treatment planning to minimize the deleterious effect of treatment setup error *Int. J. Radiat. Oncol. Biol. Phys.* **38** 199–206